

# Self-nanoemulsifying Drug Delivery System of Mebendazole for Treatment of Lymphatic Filariasis

MONICA R. P. RAO\*, SNEHA P. RAUT, C. T. SHIRSATH, MONALI B. JADHAV, AND PRANOTI A. CHANDANSHIVE

Department of Pharmaceutics, AISSMS College of Pharmacy, Pune-411001, India

Rao *et al.*: Self-nanoemulsifying Drug Delivery System of Mebendazole

Lipid-based self-nanoemulsifying drug delivery system was explored to improve the oral bioavailability and target specificity of mebendazole for treatment of lymphatic worm infestations. Ternary phase diagrams were constructed to select suitable oil-surfactant mixture. Liquid self-nanoemulsifying drug delivery system consisting of Capmul MCM L8, Chromophore RH40 and tocopherol polyethylene glycol succinates a pre-concentrate was systematically optimized using 32 full factorial designs.  $\beta$ -cyclodextrin-based nanosponges were used to prepare solid self-nanoemulsifying drug delivery system. Characterization of liquid self-nanoemulsifying drug delivery system was carried out using percent transmission, globule size, zeta potential, polydispersity index and drug content. Globule size in the range of 50-90 nm and zeta potential of -5 to -12 mV was obtained, which co-related well with percent transmission. Powder X-ray diffraction, differential scanning calorimetry and scanning electron microscope of solid self-nanoemulsifying drug delivery system indicated the presence of mebendazole as a molecular dispersion. *Ex vivo* studies showed nearly five-fold increase in the flux. *In vivo* studies showed two-fold increase in bioavailability. Significant enhancement in drug dissolution and saturation solubility from solid self-nanoemulsifying drug delivery system resulted in an increase in the bioavailability. Besides this, greater surface area, improved release, P-gp modulation potential of excipients and lymphatic bypass via Peyer's patches protected drug from hepatic first pass metabolism all of which would contribute to the observed improved bioavailability. Lymphatic transport of drug could achieve target specificity in lymphatic filariasis.

**Key words:** Mebendazole, Capmul MCM L8, TPGS, Cremophor RH40,  $\beta$ -CD nanosponge

More than 127 million people are infested by lymphatic filariasis, a mosquito-borne disease and about 1.2 billion people are at risk of the disease in 70 countries. It is most common in Africa and Asia. Lymphatic filariasis is caused by parasites, *Wuchereria bancrofti*, *Brugia malayi* and *Brugia timori*. These infest the lymph channels and disrupt the flow of the lymph leading to lymph oedema<sup>[1]</sup>. The chronic phase is marked by lymph varices (dilation of vessels), lymph scrotum, hydrocele, chyluria and elephantiasis<sup>[2]</sup>. Another form of systemic infestation is caused by the larva form of *Necator americanus*, which penetrates human skin and travels through the blood vessels to reach the pulmonary alveoli and travels up the trachea. Once it enters in lymph nodes, the larvae starts entering the blood, lungs and intestines. The therapy for these and other similar conditions comprises benzimidazoles, specifically albendazole and pyrantel pamoate<sup>[3]</sup>.

Self-nanoemulsifying drug delivery system (SNEDDS) is a novel drug delivery system with numerous

advantages including ease of production, improvement of drug solubility and oral bioavailability. SNEDDS are preconcentrates composed of isotropic mixtures of oils, surfactants and co-surfactants, which spontaneously form fine oil in water (o/w) emulsion *in situ* upon contact through aqueous medium with a globule size in the range of 20-200 nm<sup>[4]</sup>. Various other potential features of SNEDDS in improving oral bioavailability of lipophilic drugs consists of simplifying transcellular and paracellular absorption, decreasing cytochrome-P450 metabolism in the gut enterocytes, stimulating lymphatic transport via Peyer's patches and protecting drug from hepatic first pass metabolism<sup>[5]</sup>. The major drawbacks of liquid-

This is an open access article distributed under the terms of the Creative Commons Attribution-NonCommercial-ShareAlike 3.0 License, which allows others to remix, tweak, and build upon the work non-commercially, as long as the author is credited and the new creations are licensed under the identical terms

\*Address for correspondence

E-mail: monicarap\_6@hotmail.com

Accepted 30 September 2018

Revised 29 March 2018

Received 27 June 2017

Indian J Pharm Sci 2018;80(6):1057-1068

SNEDDS (L-SNEDDS) include chemical instability, precipitation of drugs at storage temperature due to loss of the volatile components or absorption of the formulation by gelatine capsule shell, leakage, high production cost. These were overcome by adsorbing them on to highly porous carriers and converting them into solids without affecting self-nanoemulsifying properties<sup>[6]</sup>.

Mebendazole (MEZ) is a broad-spectrum anthelmintic drug, which is effectual in the control of a number of nematodal and cestodal species. The principal mode of action is to inhibit tubulin polymerization, which results in loss of cytoplasmic microtubules<sup>[7]</sup>. It is highly lipophilic (log P: 2.83) with low solubility (71.3 mg/l) and undergoes extensive first pass metabolism. It has low absolute oral bioavailability (approximately 10 %) with half-life of 2.5 to 5.5 h in patients with normal hepatic function. Primary reasons for poor oral bioavailability of MEZ are hepatic first pass metabolism, low water solubility and excessive protein binding<sup>[8]</sup>. Extensive review of literature disclosed lack of information about the bioavailability enhancement of poorly water-soluble MEZ using SNEDDS. Thus the current study was aimed to develop and evaluate SNEDDS of MEZ using suitable oil-surfactant combinations and to convert L-SNEDDS into solid form. The MEZ-loaded L-SNEDDS formulations were evaluated for globule size, zeta potential, polydispersity index (PDI), self-nanoemulsification time (SEF time), thermodynamic stability of the emulsion and *in vitro* drug release. The optimized L-SNEDDS was adsorbed on solid inert carrier and evaluated for solid state characterization, *in vitro* drug dissolution behaviour and oral bioavailability in Wistar rats.

## MATERIALS AND METHODS

MEZ was gifted by Shalini Pharmaceuticals, Pune. Capmul MCM L8, Capmul MCM, Capmul MCM C8, Capmul PG, Capmul 908 P, Acconon C6, Acconon E, Captex-200, Captex 355 were gifted by Abitec Corporation, USA. Capryol 90 was gifted by Colorcon Private Ltd., Mumbai, India. Saflower oil, isopropyl myristate, polyethylene glycol (PEG)-400, propylene glycol, Cremophor RH 40, Tween 80, Tween 20, Acrysol, Pluronic F68 were purchased from S.D. Fine Chem Limited, Mumbai, India. Cremophor RH40-tocopherol polyethylene glycol succinate (TPGS) was gifted by Isochem, France. Cremophor ELP was gifted by BASF Corporation.

## Solubility studies:

Saturation solubility of MEZ was determined using shake flask method in various oils, surfactants and co-surfactants<sup>[9]</sup>. Excess amount of drug was mixed with 1 g of chosen vehicles in 5 ml clean glass vials. The mixture was heated in a water bath at 40° to facilitate the solubilisation and mixed using a cyclomixer. The dispersions were equilibrated by shaking in an orbital shaker (Remi Laboratories, Mumbai, India) at 25° for 48 h. Samples were centrifuged at 3000 rpm for 20 min and the aliquots of supernatant were analysed at 291 nm using UV/Vis double-beam spectrophotometer (Lab India UV 3000+).

## Construction of the ternary phase diagram:

The occurrence of self-nanoemulsifying oil formulation region was identified by ternary phase diagrams of systems containing oil-surfactant-co-surfactant (Smix) using water titration method<sup>[10]</sup>. Different mixtures of oil and Smix were prepared (1:9, 2:8, 3:7, 4:6, 5:5, 6:4, 7:3, 8:2 and 9:1) in pre-weighed vials. Different ratios of Smix as 1:1, 2:1, 3:1, 4:1, 1:0.5 and 1:0.75 were studied. The coordinates of the ternary phase diagram represent three components of nano emulsion system i.e., oil phase, Smix and water. Deionized water was added drop-wise to the mixtures till appearance of turbidity. The resultant mixtures were observed visually for phase clarity and flow ability. Phase diagram was constructed by using Chemix software, Chemix School Ver. 3.50 software (MN, USA, Trial version).

## Factorial study:

A 3<sup>2</sup> factorial design was employed to explore the effect of independent variables on L-SNEDDS. Based on preliminary studies, concentration of Smix and oil were selected as independent variables. The level of concentration of Smix in the formulation was varied from 6.5, 7 and 7.5 mg/ml, while levels for concentration of oil were selected to be 2.5, 3 and 3.5 mg/ml. The nine batches (B1-B9) predicted by the optimization software were analysed for particle size and zeta potential. Design Expert software version 9.0 was used for optimization. Optimized batch was selected from solutions given by software on the basis of constraints provided to software and 3D responses for all the 5 responses (droplet size, zeta potential, PDI, percent transmittance and drug content). The responses of all the nine runs were fitted in the quadratic polynomial model. The appropriate fitting model for each response was selected based on the difference of numerous statistical parameters such as R<sup>2</sup>, sequential

model sum of squares and partial sum of square given by the analysis of variance.

### Preparation of L-SNEDDS:

Based on the saturation solubility studies, vehicles having good solubilisation capacity for MEZ were selected. Nine formulations were prepared containing different compositions of Smix (TPGS) and oil (Capmul MCM L8; Table 1). L-SNEDDS were prepared by incorporating 10 mg drug into mixture of accurately weighed quantity of Smix and oil and these components were mixed and heated to 40° on a water bath to form homogenous mixture and stored at room temperature for further evaluation. The L-SNEDDS were observed for homogeneity or any change in colour, transparency or phase separation throughout normal storage condition (37±2°).

### Characterization of L-SNEDDS:

Factorial batches were analysed for globule size, zeta potential, percent transmission, drug content and optimized batch was further analysed for dispersibility, cloud point measurement and thermodynamic stability studies.

### Globule size, zeta potential and PDI:

Photon correlation spectrometer (Zetasizer, Malvern Instruments) was used to determine droplet size. The formulation (0.1 g) was diluted with 50 ml of distilled water in a volumetric flask. The flask was inverted and shaken mildly to form a fine nano-emulsion and permitted to stand for 12 h at room temperature<sup>[11]</sup>. The mean droplet size, PDI and zeta potential of the dispersions were analysed.

### Transmission test:

The clarity of the nano-emulsions was determined by measuring percent transmittance at 533 nm using UV/Vis double-beam spectrophotometer. In this study

100 mg of formulations were diluted to 100 ml with distilled water and analysed for transparency. The studies were conducted in triplicate.

### Drug content:

L-SNEDDS (100 mg) were dissolved in 10 ml methanol and vortexed. The solutions were filtered using 0.45 µm membrane filters. The drug content was estimated at 291 nm using UV/Vis double-beam spectrophotometer.

### Dispersibility studies:

The dispersibility studies were carried out to detect the self-nanoemulsification efficiency and SEF time. One millilitre of optimized L-SNEDDS batch was added to 500 ml of distilled water with gentle agitation using a magnetic stirrer at 50 rpm with temperature at 37°. Self-nanoemulsification was visually monitored for the rate of emulsification and appearance.

### Cloud point measurement:

L-SNEDDS was diluted with distilled water in the ratio 1:100 and placed in a water bath, and the temperature increased gradually. Cloud point was measured as the temperature at which there was a sudden appearance of cloudiness as seen visually<sup>[12]</sup>.

### Preparation of S-SNEDDS:

The optimized L-SNEDDS was converted into solid form by adsorption method<sup>[13]</sup> using various adsorbents like microcrystalline cellulose, calcium carbonate, magnesium carbonate, Aerosil 200 and β-cyclodextrin (β-CD) cross-linked with diphenyl carbonate (DPC) nanosponges<sup>[14,15]</sup>. β-CD and DPC (1:4) were heated to 90° for 5 h to enable the crosslinking of β-CD with carbonyl group. The synthesized product was washed with distilled water and acetone to remove unreacted β-CD and DPC. The formulation was added drop-wise onto the solid adsorbents in various ratios

**TABLE 1: EXPERIMENTAL RUN AND RESPONSES FOR OPTIMIZATION OF L-SNEDDS FORMULA USING 3<sup>2</sup> FACTORIAL DESIGNS (n=3)**

Batches	Smix (mg)	Oil (mg)	Droplet size (nm)	Zeta potential (mV)	PDI	Percent transmission	Drug content (%)
B1	6.5	2.5	95 (3.2)	-11.41 (1.5)	0.42 (0.11)	89 (1.8)	76 (1.9)
B2	7	2.5	88 (2.1)	-4.25 (0.9)	0.48 (0.09)	95 (1.7)	89 (2.3)
B3	7.5	2.5	48.4 (2.8)	-12.43 (1.6)	0.69 (0.12)	95 (1.4)	91.6 (1.4)
B4	6.5	3	79.5 (3.2)	-9.13 (2.3)	0.38 (0.08)	88 (1.6)	75 (2.4)
B5	7	3	71.5 (1.4)	-3.07 (1.24)	0.45 (0.09)	97 (2.1)	87.6 (1.3)
B6	7.5	3	52.2 (2.6)	-9.84 (1.11)	0.65 (0.1)	95 (3.7)	92 (1.5)
B7	6.5	3.5	84.4 (3.3)	-9.13 (2.1)	0.35 (0.05)	85 (1.5)	82 (1.3)
B8	7	3.5	75 (1.4)	-2.25 (1.1)	0.42 (0.1)	94 (1.7)	90.1 (1.3)
B9	7.5	3.5	65.8 (1.6)	-11.45 (2.3)	0.63 (0.2)	92 (2.1)	99.4 (2.3)

Values in parentheses indicate SD. Smix- Cremophor RH40:TPGS. Oil- Capmul MCM L8

(1:1, 1:2 and 1:3). After each addition, the mixture was homogenized by trituration to ensure uniform distribution of the droplet. The adsorbent that gave free flowing S-SNEDDS was selected for further studies.

### **Micromeritic properties:**

Micromeritic properties of S-SNEDDS were determined by angle of repose, Carr's index (CI) and Hausner's ratio<sup>[16]</sup>. Content of one capsule of S-SNEDDS was reconstituted in 50 ml of distilled water, allowed to stand for 12 h at room temperature and the droplet size of the emulsion was measured as per the procedure stated under L-SNEDDS. The DSC thermogram of pure MEZ and S-SNEDDS was recorded using (Mettler Toledo DSC 823e, Japan). Approximately 5 mg of sample was heated in a closed pierced aluminium pan from 30° to 180° at a heating rate of 5°/min under a stream of nitrogen at a flow rate of 50 ml/min. The outer macroscopic structures of nanosponges and S-SNEDDS were investigated by scanning electron microscope (JSM-6360A, Jeol, Tokyo, Japan) at an accelerating voltage of 15 kV. The particles were previously fixed on a carbon stub using double-sided adhesive tape and then were made electrically conductive by thin platinum coating (3-5 nm), in vacuum for 100 s at 30 W. Powder X-ray diffraction pattern of pure MEZ and S-SNEDDS was investigated using powder X-ray diffractometer (PW 1729 X-ray Generator, Philips, Netherlands). The X-rays were Ni filtered CuK $\alpha$ 1 radiation with 40 kV and 30 mA over 0-100°/2 $\theta$ .

### ***In vitro* dissolution studies:**

*In vitro* dissolution studies were conducted by dialysis bag method using the dialysis bag (Himedia LA 401, 1000KD) for both L-SNEDDS and S-SNEDDS<sup>[17,18]</sup>. SNEDDS equivalent to 10 mg of MEZ was filled in a pouch fashioned out of the dialysis bag and subjected to dissolution studies using USP dissolution type-II apparatus with 500 ml of phosphate buffer (pH 6.8) at 50 rpm set at 37 $\pm$ 0.5°. No enzymes were added to the media. At predetermined time intervals, aliquots of 5 ml were collected and replaced with fresh dissolution medium. The samples were analysed using UV method at 291 nm.

### **Permeation studies using everted intestinal sac:**

Everted intestinal sac method was used to study the absorption across intestinal membrane. The rat was sacrificed and the intestine was carefully manoeuvred so as to remove the mesenteric attachments without

damaging the intestinal architecture. A length of 8-10 cm was removed and washed carefully with normal saline (0.9 % w/v NaCl). Intestine was everted over a glass rod and placed in a flat dish containing Krebs-Henseleit bicarbonate buffer at 37°. The apparatus consisted of a U tube glass chamber with a break in one arm to facilitate the mounting of the everted intestine. This entire assembly was clamped and placed in the dissolution vessel. The inside of the U tube serves as the intestinal lumen and the dissolution vessel serves as the serosal compartment. Krebs solution (900 ml) was used as dissolution media and S-SNEDDS were subjected to permeation studies at 37° and 50 rpm stirring speed in the USP type II dissolution apparatus. The aliquots were collected at different time points (every 10 min for 1 h) and analysed by UV spectroscopy at 291 nm<sup>[19]</sup>.

### **Pharmacokinetic studies:**

Approval of Institutional Animal Ethics Committee bearing Approval No: CPCSEA/IAEC/PT-06/01-2K16, was obtained for performing pharmacokinetic studies. Male Wistar rats, about 250-300 g were fasted for 24 h with free access to water. The animals were divided into 2 groups of 6 rats in each group *viz.* the first group, which was administered pure MEZ, and the second group was administered S-SNEDDS suspension orally using a feeding tube (equivalent to 10 mg/kg dose). Blood (0.5 ml) was withdrawn at intervals of 30 min for 5 h from the retro orbital vein, with the help of insulin syringe and analysed by reversed-phase high-performance liquid chromatography (RP-HPLC) on a C18 (150 $\times$ 4.6 mm i.d.; 5  $\mu$ m particle size) column. The mobile phase comprised of acetonitrile:phosphate buffer (55:45 v/v) adjusted to pH 6.5 with ortho-phosphoric acid, with a flow rate of 1.2 ml/min<sup>[20]</sup>.

## **RESULTS AND DISCUSSION**

Solubility studies were performed for selection of oil phase so as to determine individual solubilisation capacity of each oil phase for drug under investigation as it is an important consideration for oil phase selection. To achieve optimum drug loading in self-nanoemulsifying formulations, identification of suitable oil, surfactant/co-surfactant having maximal solubilizing potential for drug is very important<sup>[21]</sup>. The saturation solubility of MEZ was determined in long chain triglycerides (LCT) such as safflower oil and in medium chain triglycerides (MCT) such as Capmul MCM L8, Capmul MCM, Capmul MCM C8, Capmul PG, Capmul 908 P (fig. 1A). Capmul MCM L8 was selected as the oil phase owing to its higher solubilisation



capacity and ease of self-nano-emulsification. Capmul MCM L8 is chemically monoglycerides of caprylic acid, which contains caprylic acid about 97 % and capric acid 3 %. Caprylic acid is an unsaturated fatty acid having capacity to improve bioavailability<sup>[22]</sup>. The higher solubility in MCT than LCT is seen due to the higher ester bond content per gram of the MCT<sup>[4]</sup>. Rane and Anderson<sup>[23]</sup> have reported that a certain degree of polarity present in a lipid with lower chain lengths is required to solubilize drug as there could be an interaction between hydrophilic head groups of the lipids and polar moieties in the drug. Capmul MCM L8, being a monoglyceride can be presumed to be relatively hydrophilic than its corresponding diglyceride and could be considered to have required hydrophilic-lipophilic balance to solubilize MEZ. Selection of surfactant is also critical for a self-nanoemulsifying formulation as it forms a thin film at the interface, decreases the globule size, helps in stabilization of the emulsion and exerts absorption enhancing effect by partitioning into the cell membrane and enhances permeation<sup>[24]</sup>. Only hydrophilic surfactants (HLB>12) were screened, as they favour the formation of o/w emulsion. Non-ionic surfactants such as Cremophor RH 40, Tween 80, Tween 20, Acrysol, Pluronic F68, TPGS, Captex 200, PEG 400, Captex 355, propylene glycol, Acconon E and Acconon C6 were investigated because of their lower toxicity as compared to ionic

surfactants (fig. 1B). Among all the surfactants, Cremophor RH40 was found to have maximum solubilisation capacity for the drug. Cremophor RH40 is polyoxyl-40 hydrogenated castor oil. Its amphiphilic nature, ability to dissolve large quantity of drugs and good self-nano-emulsification property makes it suitable for lipid-based formulations<sup>[25]</sup>.

Nanoemulsion formation is a dynamic process, which involves exchange of water between bound to free states, exchange of co-surfactant from the interfacial film to continuous phase and dispersed phase and exchange of surfactant between the interfacial film and water. This dynamic behaviour is offered due to presence of co-surfactant, which imparts flexibility of the interfacial film in nanoemulsion<sup>[26]</sup>. As MEZ was found to have maximum solubility in TPGS and Acconon, these were screened as co-surfactants. TPGS is an amphiphile with a low critical micelle concentration (CMC). Its lipophilic and hydrophilic portions are bulky and have large surface areas, which make it a good emulsifier<sup>[27]</sup>. Acconon C6 is a polyoxyethylene 6 caprylic glyceride known as water-soluble emollient. It is nonionic and compatible with other ionic species and is widely used as an emulsifying agent with an HLB of 12.5<sup>[28,29]</sup>.

Besides this, number of studies have been reported wherein TPGS has synergistically contributed to the stability of nano systems. TPGS works as steric stabilizer along with polyvinylpyrrolidone and decreases interfacial tension between the nanoparticles, thus minimizing aggregation<sup>[28]</sup>. Besides this, Shukla *et al.* studied Acconon C6 as a co-surfactant, which improved the solvent capacity of the formulation, stability and oral bioavailability of candesartan cilexetil<sup>[30]</sup>.

Pseudo ternary phase diagrams were constructed to identify the self-nanoemulsifying regions. Selection of oil, Smix, and the ratio of Smix play an important role in the formation of the nanoemulsion. The free energy for formation of nanoemulsions depends on the extent of decrease in o/w interfacial tension and the change in dispersion entropy<sup>[31]</sup>. Ternary phase diagrams (fig. 2) were constructed with different Smix ratios of 1:1, 2:1, 3:1, 4:1 for two Smix combinations of Cremophor RH40-Acconon C6 (Smix<sub>1</sub>) and Cremophor RH40-TPGS (Smix<sub>2</sub>). For Smix<sub>2</sub>, additional ratios of 1:0.5 and 1:0.75 were also investigated. Nanoemulsion region for Smix<sub>2</sub> (1:0.5) was found to be greater than all other ratios of both Smix. Ternary diagram for Smix<sub>1</sub> showed increasing nano-emulsion region with

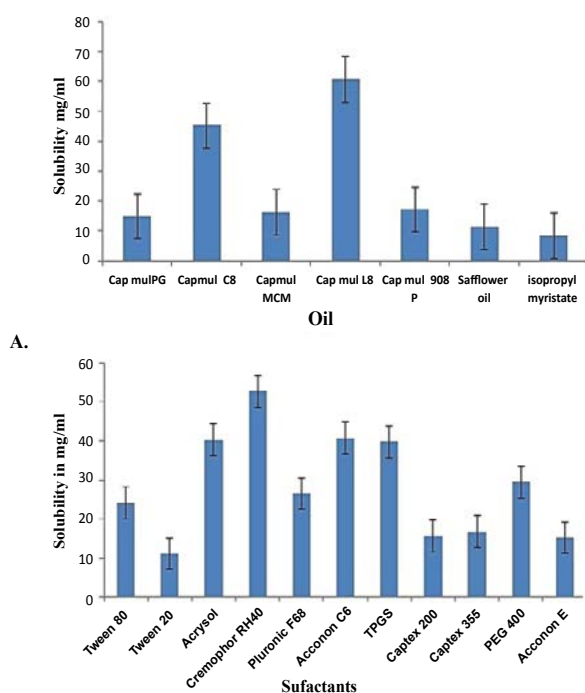


**Fig. 1: Saturation solubility of MEZ**  
Saturation solubility of mebendazole (MEZ) (A) in oils and (B) surfactants and co-surfactants

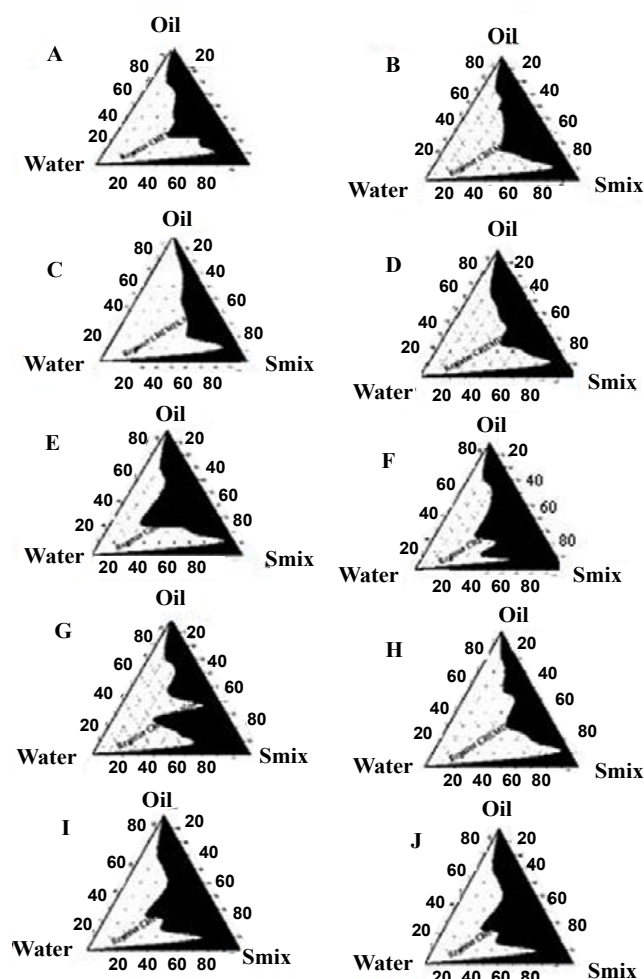


**Fig. 2: Ternary phase diagrams for nanoemulsions**  
 Smix1: Cremophor:Acconon C6 ratios A- 1:1, B- 2:1, C- 3:1, D- 4:1. Smix2: Cremophor:TPGS ratios E- 1:1, F- 2:1, G- 3:1, H- 4:1, I- 1:0.5, J- 1:0.75

increments in concentration of the Cremophor RH40 up to a ratio of 1:3, but at the ratio of 4:1, highly viscous gel was formed. This could be due to formation of liquid crystalline phase of Cremophor RH40. As the concentration of surfactant with respect to co-surfactant increases, nanoemulsion region increases because large amount of Smix form tightly packed interfacial film resulting in reduced droplet size and better stability<sup>[32]</sup>. When there are sufficient numbers of micelles in solution phase, they start to pack together in a number of geometric structures known as liquid crystals. Liquid crystals have the ordered molecular arrangement of solid crystals; they increase the viscosity of the solution phase<sup>[23]</sup>, which may explain the formation of gel-phase at higher concentration of Cremophor RH40.

In the case of Smix<sub>2</sub>, marginal differences were observed in the nanoemulsion areas. However as TPGS is a semisolid at room temperature, all combinations of

Smix<sub>2</sub> except 1:0.5, were highly viscous. This property may have a profound effect on the handling and self-emulsification properties of the SNEDDS.

The pre-concentrates of Smix<sub>1</sub> combinations comprised total surfactant concentration ranging from 20 to 50 % whereas for Smix<sub>2</sub> pre-concentrates the total surfactant concentration ranged from 15 to 50 %. It was observed that Smix<sub>2</sub> at 15 % concentration gave almost similar nanoemulsion region as compared to 40 % Smix<sub>1</sub> and hence Smix<sub>2</sub> at 1:0.5 ratios (15 % w/w) was selected for further studies.

A 3<sup>2</sup> full factorial study was employed for the systematic optimization of the SNEDDS. The ranges for oil, surfactant and co-surfactant for optimized batch were provided by the software based on the responses generated in the factorial batches (B1-B9) and the input constraints of the target responses viz. droplet size, zeta potential, PDI, percent transmittance and drug content. The optimized batch was evaluated for various responses and compared with the predicted responses.

The droplet size of the emulsion is a crucial factor in self-nano-emulsification performance because it determines the rate and extent of drug release as well as absorption<sup>[33]</sup>. As can be seen from fig. 3 droplet size decreased as surfactant concentration increased, which can be attributed to stabilization of the oil droplets. The average droplet size of nanoemulsions B1-B9 ranged between 49 to 95 nm. Higher globule size was evident at decreasing Smix concentration and increasing oil content whereas smaller oil droplets would mean larger oil-water interfacial area thereby necessitating greater amount of Smix to stabilize the droplets<sup>[16]</sup>. Eqn. 1, droplet size = +72.59–15.42 A–1.03 B+7 AB–7.28 A<sup>2</sup>+8.37B.

The higher and negative coefficient for factor A (Smix concentration) in the polynomial Eqn (Eqn. 1) is indicative of decrease in droplet size with increase in Smix concentration. The model F-value of 11.06 implied that the quadratic model is significant. The  $p < 0.05$  for the terms A, B, A<sup>2</sup> and B<sup>2</sup> indicated significant and exponential effect of the terms on the globule size (Table 2).

Zeta-potential for all the formulations was found to be –2 to –12 mV. The negative zeta potential of all batches could be attributed to the ionization of surface functional groups of oil especially the free carboxylic acid groups. An increase of electrostatic repulsive forces prevents the coalescence of nanoemulsion droplets<sup>[34]</sup>. However, the small negative zeta potential

values of L-SNEDDS could be due to the ionization of free fatty acids and glycols present in the oil and surfactants, which improves stability by preventing globule coalescence<sup>[35]</sup>. Eqn. 2: zeta potential =  $2.43 - 0.67 A + 0.88 B - 0.32 AB - 7.37 A^2 - 1.14 B^2$ .

As can be seen from fig. 3, zeta potential showed a decrease with decreasing in Smix concentration and increase with increasing oil concentration. Similar effect was seen in every coefficient. The interaction term AB shows a feeble lowering on zeta potential value. The model F-value of 56.09 implies the quadratic model is significant and A, B are significant model terms shown in Table 2. The PDI was found to be in between 0.23 to 0.45. Higher polydispersity is indicative of non-uniform droplet size distribution. Greater uniformity of globule (low PDI) is essential for long term nanoemulsion stability<sup>[36]</sup>. Eqn. 3:  $PDI = 0.45 + 0.14 A - 0.032 B + 2.500E-003 AB + 0.070 A^2 + 5.00E-003 B^2$ .

Smix concentration showed a positive effect on PDI in comparison with oil concentration (fig. 3). The model F-value of 1842.60 implied that the quadratic model is significant. In this case A, B, A<sup>2</sup> were found to be significant model terms (Table 2).

Percent transmittance test is indicative of the robustness of the formulations to dilution. All the formulations showed percent transmittance above 90 %, which indicated that the droplet size was in nm range. Nanoemulsions appear optically transparent, even at large phase volume ratio and for large difference in refractive index. Nanoemulsions may lose their transparency with time as a result of increase in droplet size<sup>[34]</sup>. This in turn provides a large surface area for the drug release and absorption in the GI tract<sup>[37]</sup>. The data shows that percent transmission increases with increase in Smix concentration and decreases with decrease in oil concentration (fig. 3). Eqn. 4: % transmittance =  $96.44 + 3.33 A + 1.33 B + 0.25 AB - 4.67 A^2 - 1.67 B^2$ . The model F-value of 26.57 implied the significance of the quadratic model. In this case A, B, A<sup>2</sup> are significant model terms (Table 2).

Percent drug content for L-SNEDDS showed higher contribution of Smix and oil. A proportionate increase in MEZ loading was observed upon increasing the concentration of oil, while the former was decreased upon decreasing the concentration of Smix at a fixed concentration of Capmul MCM L8. Eqn. 5: drug content =  $87.40 + 7.43 A + 1.58 B - 0.90 AB - 3.80 A^2 + 2.25 B^2$ .

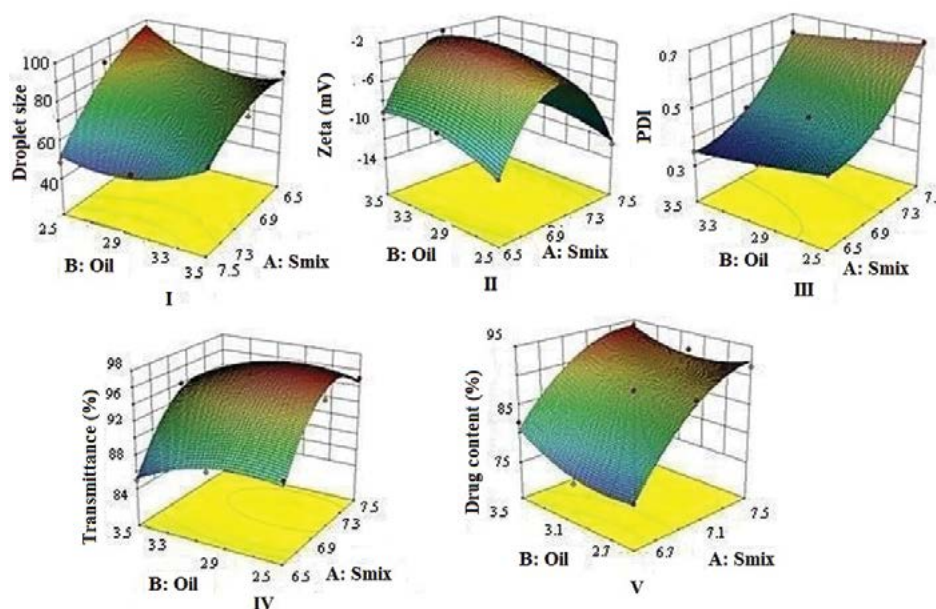


Fig. 3: 3D surface response plots

I- Droplet size, II- zeta potential, III- PDI, IV- % transmittance, V- drug content

TABLE 2: PROBABILITY VALUES FOR VARIOUS RESPONSES

Coefficient	Prob>F value				
	Droplet size (nm)	Zeta potential (mV)	PDI	% Transmission	Drug content (%)
AB	0.0955	0.3921	0.2722	0.6440	0.3150
A <sup>2</sup>	0.1750	0.0005	0.0001	0.0066	0.0369
B <sup>2</sup>	0.1350	0.0898	0.1540	0.0947	0.1232



The model F-value of 34.78 implies the quadratic model is significant. In this case  $A^2$  is significant model terms. Droplet size distribution, PDI, zeta-potential, percent transmission and drug content results are shown in Table 1. For all the responses model-F value indicated that quadratic model was significant. Based on solutions given by Design Expert software version 9.0, three optimized batches (S1, S2 and S3) were selected. L-SNEDDS (S1, S2 and S3) were prepared and evaluated for the five responses and desirability of statistical design was checked. Difference between predicted and experimental batch was found to be minimum for both batches (Table 3). The S1 batch was selected for further studies as it had better desirability and minimum percent error.

Besides the five responses, the selected optimized batch was evaluated for SEF time, cloud point and thermodynamic stability. The optimized S1 batch of L-SNEDDS prepared as per the experimental design showed good self-nanoemulsification efficiency and nanoemulsion formed within 1 min of dilution. Estimation of cloud point is an important factor for the stability of self-emulsifying formulation. The cloud point is the temperature above, which dehydration of self-emulsifying ingredients occurs and turns a clear dispersion to a cloudy one which in turn may affect drug absorption<sup>[38]</sup>. Hence, cloud point of self-emulsifying formulation should be above body temperature (37°). The cloud point of S1 batch was found to be 74°, indicating that the nano emulsion will maintain its integrity at physiological temperature.

L-SNEDDS are generally filled in soft gelatin capsules for end use. However problems of leaching of oil or surfactant are possible over long term storage. Hence conversion of L-SNEDDS to solid state offers a convenient alternative, which also simultaneously improves the handling properties. The S-SNEDDS can be incorporated into capsules directly or

transformed into granules, pellets and powders for tablet preparations. Adsorption of the pre-concentrate onto various adsorbents offers good content uniformity as well as improved handling properties<sup>[39,40]</sup>. Various adsorbents were studied in the present work to convert the optimized L-SNEDDS to solid form. Besides the conventional adsorbents like microcrystalline cellulose, calcium carbonate, magnesium carbonate and Aerosols 200,  $\beta$ -CD-based nanosponges were used to load the L-SNEDDS. Nanosponges have been previously studied for their adsorbent properties in non-pharmaceutical fields. Moura and Lago<sup>[41]</sup> studied the catalytic growth of carbon nanotubes and nanofibers on vermiculite to produce floatable hydrophobic “nanosponges” for oil spill remediation<sup>[42]</sup>.

In earlier studies,  $\beta$ -CD nanosponges were used for enhancement of permeation (curcumin)<sup>[43]</sup>, solubility (cefpodoxime proxetil)<sup>[44]</sup>, stability (camptothecin)<sup>[45]</sup>, for taste masking (gabapentin)<sup>[46]</sup> and for controlled release (telmisartan)<sup>[47]</sup>. The adsorbent that was required in a small amount and gave a free flowing S-SNEDDS was selected for further study. It was observed that nanosponges had superior adsorption capacity than other adsorbents. This may be due to its porous nature, crosslinking and lipophilic interior cavities<sup>[48]</sup>.

Various physical interactive forces such as van der Waals forces could play a role in adsorption of the L-SNEDDS onto nanosponges. Besides this the pores could be providing additional interfaces for entrapping the oil-drug-Smix combination<sup>[49]</sup>. Other adsorbents gave free flowing powder in the ratio of 1:3 whereas nanosponges formed free flowing powder in the ratio was 1:2 (L-SNEDDS: nanosponge). So, L-SNEDDS were adsorbed on to nanosponges and further evaluated. The S-SNEDDS showed good flow property with CI of 18, Hauser's ratio of 1.25 and angle of repose of 27°. These findings indicated good packing ability, which may be attributed to spherical nature of particles. The droplet size of reconstituted S-SNEDDS was found

**TABLE 3: VALIDATION OF OPTIMIZED BATCHES (n=3)**

A	Globule size (nm)			Zeta potential (mV)			PDI		
	S1	S2	S3	S1	S2	S3	S1	S2	S3
Predicted value	54.34 (3.2)	56.51 (2.8)	55.21 (3.2)	-11.3 (1.5)	-10.5 (1.9)	-11.6 (1.9)	0.67 (0.08)	0.65 (0.12)	0.68 (0.11)
Observed value	54.98 (2.1)	57.21 (3.2)	57.13 (2.9)	-11.8 (1.7)	-11.0 (1.5)	-10.5 (2.5)	0.70 (0.11)	0.69 (0.22)	0.67 (0.39)
% error	0.51	0.7	0.78	0.028	0.52	0.66	0.25	0.34	0.26
B	Percent transmission			Percent drug content					
	S1	S2	S3	S1	S2	S3			
Predicted value	94.86 (1.8)	95.19 (1.7)	94.21 (3.2)	92.54 (1.9)	92.46 (1.5)	93.31 (1.9)			
Observed value	95.12 (1.4)	95.63 (1.5)	92.13 (2.9)	92.94 (2.1)	93.21 (2.3)	92.50 (2.5)			
% error	0.39	0.43	0.78	0.42	0.92	0.66			

Values in parentheses indicate SD



to be 68 nm, which signifies a marginal increase. The self-emulsification time for S-SNEDDS was found to be 50 s.

DSC thermograms of pure MEZ and S-SNEDDS were presented in fig. 4A. Pure MEZ showed a sharp endothermic peak at about 260°, which was followed by the second endotherm at 320°, which indicated its crystalline nature (curve A). MEZ is reported to exist in three polymorphic forms i.e., A, B and C with marginal differences in their solubility profile<sup>[50]</sup>. In the present study the polymorph C was provided by the company as gift sample. No MEZ peak was evident in the S-SNEDDS (curve B), indicating that MEZ was present in molecularly dissolved state in the nanosponges. X-ray powder diffractograms (fig. 4B) for pure MEZ showed sharp peaks at 2θ angles of 10.4, 12.6, 18.5, 19.9, 20, 20.1, 25, 25.1, 25.2, 27, and 27.2° that indicated the drug was in crystalline state. A distinctive halo pattern was observed for the S-SNEDDS, which supported the DSC findings that the drug was molecularly dispersed in the oil-Smix, which retained its integrity even after adsorption on nanosponge<sup>[51]</sup>. The scanning electron micrographs of plain nanosponges and S-SNEDDS were shown in fig. 5. The sponge particles appeared spherical with a smooth, porous surface. The surface of S-SNEDDS

clearly showed the presence of the adsorbed material.

The percent cumulative drug release for L-SNEDDS was found to be 98 % in 4 h whereas S-SNEDDS showed 96 % in 4 h and that for pure drug maximum release was 39 % (fig. 6). It is reported that the nanosize of the droplets in SNEDDS will facilitate faster release rate of the drug<sup>[11]</sup>. Thus, greater availability of dissolved MEZ from the SNEDDS could lead to higher absorption and higher oral bioavailability. Initially, the MEZ release from S-SNEDDS was marginally slower than its release from L-SNEDDS. This could be due to marginal increase in diffusion path length for the drug in S-SNEDDS<sup>[52]</sup>.

Permeability in GIT of any formulation is a crucial factor, which decides absorption and bioavailability of drug from that formulation<sup>[48]</sup>. Hence *ex vivo* permeability studies were carried out to determine permeability of MEZ in intestine from S-SNEDDS and plain drug. Initially a steady increase in amount diffused was evident up to 30 min followed by sharp increase as indicated by steep slope in graph (fig. 7A). Flux for MEZ and S-SNEDDS was found to be 0.271 and 0.754 µg/cm<sup>2</sup>/min, respectively; an increase of approximately 4.8 times was evident<sup>[53]</sup>. Absorption mechanism of oil droplet of SNEDDS includes passive diffusion, pinocytosis or endocytosis. Besides this, their nanometric droplet size provides a large interfacial surface area for drug release and permeation. Besides globule size, TPGS and Cremophor RH 40 also play an important role in modifying the membrane structure thereby enhancing the permeability of the diffusant. The poor bioavailability of MEZ is attributed to P-gp efflux mechanism<sup>[7]</sup> and Cremophor RH 40 and TPGS are reported to inhibit this mechanism thereby leading to enhanced migration across intestinal membrane<sup>[48,51]</sup>.

The pharmacokinetic data (Table 4) revealed improved bioavailability of S-SNEDDS as compared to pure MEZ. S-SNEDDS showed a greater initial rate of absorption compared to pure MEZ. A two-fold increase in relative bioavailability of MEZ in S-SNEDDS was observed as compared to pure MEZ (fig. 7B). Improvement in oral bioavailability can be attributed to many factors, which in combination or alone, contribute to increase in absorption. These include presence of lipophilic drug in small emulsion globules which eliminates the dissolution step and keeps drug in a dissolved state during transport through GI membrane and lymphatic transport through intestinal transcellular pathways<sup>[54,55]</sup>. In addition, the use of Cremophor RH40 and TPGS in

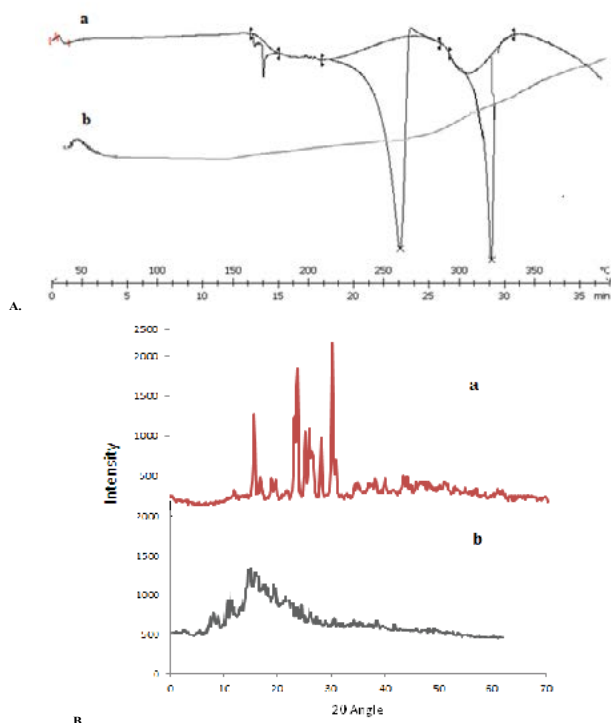


**Fig. 4: DSC curves and X-ray powder diffractograms**  
**A. DSC curves of (a) pure mebendazole and (b) S-SNEDDS and**  
**B. X-ray powder diffractograms of (a) pure mebendazole and**  
**(b) S-SNEDDS**

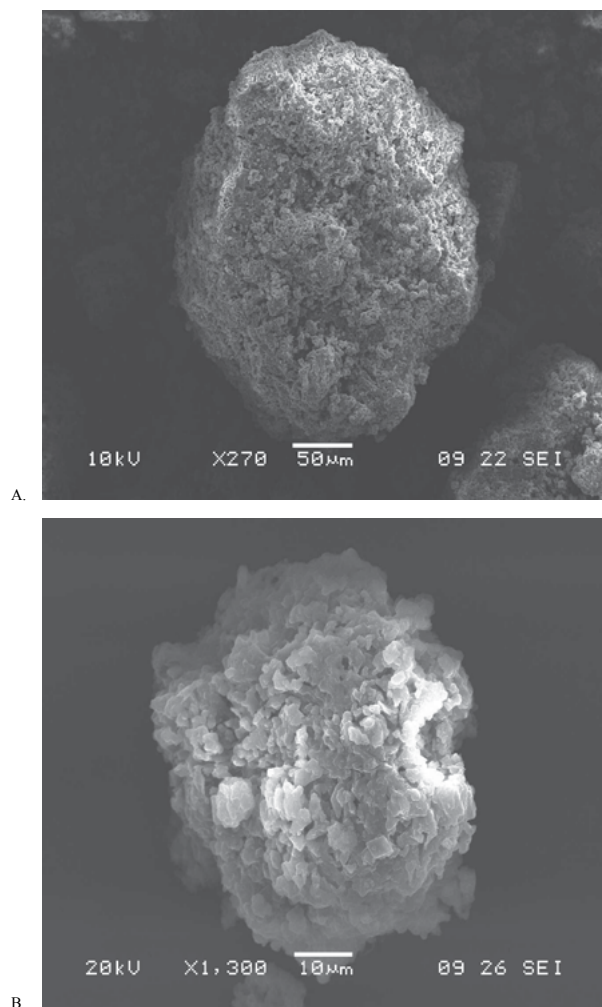


Fig. 5: SEM of (A) nanosponge and (B) S-SNEDDS

**TABLE 4: IN VIVO PHARMACOKINETIC PARAMETERS OF PURE MEZ AND S-SNEDDS IN RATS (n=3)**

Parameters	Pure MEZ	S-SNEDDS
Cmax (ug/ml)	1.24±0.12	3.38±0.21
tmax (h)	1.5	1
AUC (0-5 h) (μg/ml-h)	126.07±0.3	294.02±0.01

the formulation may modulate the P-gp efflux pumps and/or CYP450 enzymes function in the intestine region and improve the absorption of drug<sup>[48,52]</sup>. Earlier reports suggested that the majority of the lipid-based systems comprising of long chain and medium chain fatty acids gain admittance to intestinal lymph and bypass the portal circulation. This helps in treatment of helminth infestation, which affect the lymph vessels in acute and chronic phase such as lymphatic filariasis as discussed earlier. It is possible also to further presume that these systems, because of their high surfactant concentration may be able to penetrate the worms or their larval forms more efficiently. Various studies have been conducted to understand the role of surfactants

in enhanced penetration of drugs into worms and it has been proved that surfactants below their CMC increased the rate of penetration by disrupting the membrane structure of the worms<sup>[56]</sup>. Thus it could be inferred that SNEDDS would offer manifold benefits in treating lymphatic filariasis and other similar lymph conditions in terms of targeting the lymph vessels and improved penetration into the worms.

Worldwide, numerous studies have been taken up to develop effective therapy of diseases/conditions

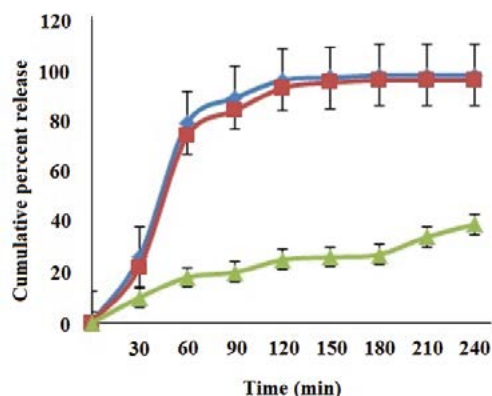
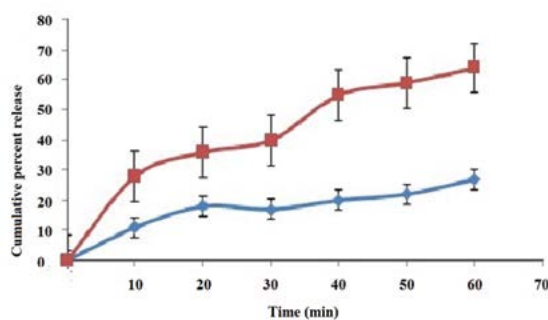
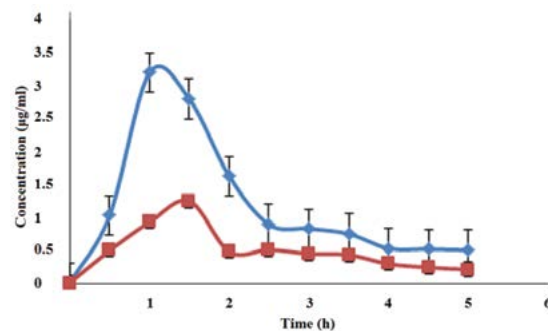


Fig. 6: *In vitro* release profile of L-SNEDDS, S-SNEDDS and MEB

Percent cumulative drug release L-SNEDDS (—◆—), percent cumulative drug release S-SNEDDS (—■—) and percent cumulative drug release from MEB (—▲—)



A.



B.

Fig. 7: *Ex vivo* diffusion and plasma concentration profiles of S-SNEDDS and MEB

(A) *Ex vivo* diffusion and (B) plasma concentration profile of S-SNEDDS and MEB, In the panel A, MEB (—◆—) and S-SNEDDS (—■—). In the panel B: concentration in μg/ml of S-SNEDDS (—◆—) and concentration of MEB in μg/ml (—■—)

like diabetes as well as AIDS and cancer. However certain debilitating conditions/infections are prevalent in tropical countries, which require concerted efforts to improve therapy and efficacy. The WHO has identified lymphatic filariasis as one of the neglected infection affecting a large chunk of African and Asian population. In the present study, an attempt was made to improve efficacy of MEZ, a BCS class IV drug, which is commonly prescribed for treating worm infestations afflicting the lymphatic system. The significant increase in drug dissolution and saturation solubility from S-SNEDDS resulted in increase in bioavailability. Besides this, greater surface area, improved release, P-gp modulation potential of excipients and lymphatic bypass via Peyer's patches protects drug from hepatic first pass metabolism, which will contribute to improved bioavailability. Since lipid-based systems exhibit lymphatic transport, it is possible to presume target specificity for this drug delivery for treating lymphatic infestations like filariasis. Future work could be directed towards development of S-SNEDDS for other similar drugs or their combinations to achieve improved efficacy and better therapy.

### Acknowledgements:

The authors would like to thank Dr. Ashwini Madgulkar Principal, AISSMS College of Pharmacy, Pune, India for providing necessary facilities to carry out the research work.

### Conflict of interest:

The author's report no declaration of interest, financial or otherwise regarding this project.

### REFERENCES

1. Lymphatic filariasis. (Accessed on 2017 June 21). Available from: <http://www.who.int/mediacentre/factsheets/fs102/en/>.
2. Reddy M, Gill S, Kalkar S. Oral drug Therapy for multiple neglected tropical diseases, A systematic review. JAMA 2007;298(16):1911-24.
3. Bethony J, Brooker S, Albonico M, Geiger SM, Loukas A, Diemert D, *et al*. Soil-transmitted helminth infection: ascariasis, trichuriasis, and hookworm. Lancet 2006;367:1521-32.
4. Pouton C, Porter C. Formulation of lipid-based delivery systems for oral administration, materials, methods and strategies. Adv Drug Deliv Rev 2008;60(6):625-37.
5. Date AA, Desai N, Dixit R, Nagarsenker M. Self-nano-emulsifying drug delivery systems, Formulation insights, applications and advances. Nanomedicine 2010;5(10):1595-616.
6. Shinde G, Kuchekar S, Kamble P, Kuchekar A, Kshirsagar R. Self-micro-emulsifying drug delivery system, A novel approach for hydrophobic drug. Int J Pharm Sci 2011;3(1):988-1005.
7. AL-Budrz AA, Tariq M. Mebendazole. In Florey K, editor. Analytical profiles of drug substances. New York: Academic Press; 1987. p. 293-326.
8. Mebendazole. DrugBank. Available from: <http://www.drugbank.ca/drugs/DB00643>.
9. Zhou L, Yang L, Tilton S, Wang J. Development of a high throughput equilibrium solubility assay using miniaturized shake flask method in early drug discovery. J Pharm Sci 2007;96(11):3052-71.
10. Kang JH, Oh DH, Oh YK, Yong CS, Choi HG. Effect of solid carriers on the crystalline properties, dissolution and bioavailability of flurbiprofen in solid self-nanoemulsifying drug delivery system (solid SNEDDS). Eur J Pharm Biopharm 2012;80(2):289-97.
11. Balakrishnan P, Lee BJ, Oh DH, Kim JO, Hong MJ, Jee JP, *et al*. Enhanced oral bioavailability of dexibuprofen by a novel solid Self-emulsifying drug delivery system. Eur J Pharm Biopharm 2009;72(3):539-45.
12. Bandyopadhyay S, Katore OP, Singh B. Optimized self-nano-emulsifying systems of ezetimibe with enhanced bioavailability potential using long chain and medium chain triglycerides. Colloids Surf B Biointerfaces 2012;100:50-61.
13. Joshi M, Pathak S, Sharma S, Patravale V. Solid micro emulsion pre-concentrate (Nanosorb) of artemether for effective treatment of malaria. Int J Pharm 2008;362(1-2):172-8.
14. Trotta F, Zanetti M, Cavalli R. Cyclodextrin-based nanosponges as drug carriers. Beilstein J Org Chem 2012;8:2091-99.
15. Trotta F, Cavalli R, Tumiatti V, Zerbinati O. Ultrasound Assisted Synthesis of Cyclodextrin Based Nanosponges. World J Pharm Sci 2007;89-94.
16. Krishnarajan D, Gowthman R, Sainudeen M. Effect of cellulose and non-cellulose polymers on ciprofloxacin extended release tablets. J Chem Pharm Res 2012;4(7):3617-23.
17. Jain S, Jain AK, Pohekar M, Thanki K. Novel self-emulsifying formulation of quercetin for improved *in vivo* antioxidant potential: implications on drug induced cardiotoxicity and nephrotoxicity. Free Radic Biol Med 2013;65:117-30.
18. Zhang P, Liu Y, Feng N, Xu J. Preparation and evaluation of self-microemulsifying drug delivery system of oridonin. Int J Pharm 2008;355(1-2):269-76.
19. Pietzonka P, Walter E, Duda-Johner S, Langguth P, Merkle HP. Compromised integrity of excised porcine intestinal epithelium obtained from the abattoir affects the outcome of *in vitro* particle uptake studies. Eur J Pharm Sci 2002;15(1):39-47.
20. Parakh DR, Madagul JK, Mene HR, Patil MP, Kshirsagar SJ. RP-HPLC method development and validation for quantification of mebendazole in API and Pharmaceutical formulation. Pharma Tutor J 2016;4(5):46-51.
21. Pouton CW. Lipid formulations for oral administration of drugs: non-emulsifying, self-emulsifying and self-micro emulsifying drug delivery systems. Eur J Pharm Sci 2000;11:93-8.
22. Capmul. ABITEC Corporation, (Accessed on 23.06.17). Available from: <http://www.abiteccorp.com/.../Capmul%20MSDS/Capmul%20MCM%20L8.pdf>.
23. Rane SS, Anderson BD. What determines drug solubility in lipid vehicles: Is it predictable. Adv Drug Del Rev 2008;60(6):638-56.



24. Mohsin K, Long MA, Pouton CW. Design of lipid-based formulations for oral administration of poorly water-soluble drugs: precipitation of drug after dispersion of formulations in aqueous solution. *J Pharm Sci* 2009;98(10):3582-95.
25. CREMOPHOR® RH 40. BASF's Care Creations. (Accessed on 23.06.17). Available from: <https://www.carecreations.basf.com/product-formulations/products/products-detail/CREMOPHOR%20RH%2040/30035134>.
26. Bagwe RP, Kanicky JR, Palla BJ, Patanjali PK, Shah DO. Improved drug delivery using microemulsions: Rationale, recent progress, and new horizons. *Crit Rev Ther Drug Carrier Syst* 2001;18(1):77-140.
27. Vitamin E TPGS NF. (Accessed on 21.06.17). Available from: <http://www.parmentier.de/gpf/tpgsbrosch.pdf>.
28. Gao L, Liu G, Kang J, Niu M, Wang Z, Wang H. Paclitaxel Nano suspensions coated with P-gp inhibitory surfactants: I. Acute toxicity and pharmacokinetics studies. *Colloids Surf B Biointerfaces* 2013;111:277-81.
29. Technical Data Sheet, ABITEC Acconon® CC-6. Available from: <https://www.ulprospector.com/en/na/PersonalCare/Detail/601/24626/Acconon-CC-6>.
30. Shukla J, Ani G, Abdel W. Formulation and Evaluation of Oral Self Micro-emulsifying Drug Delivery System of Candesartan Cilexetil. *Int J Pharm Sci* 2010;2:143-6.
31. Charles L, Anthony A. Current State of Nanoemulsions in Drug Delivery. *J Biomater Nanobiotechnol* 2011;2:626-39.
32. Yi T, Wan J, Xu H, Yang X. A new solid self-micro emulsifying formulation prepared by spray-drying to improve the oral bioavailability of poorly water soluble drugs. *Eur J Pharm Biopharm* 2008;70(2):439-44.
33. Pouton CW. Formulation of poorly water-soluble drugs for oral administration: physicochemical and physiological issues and the lipid formulation classification system. *Eur J Pharm Sci* 2006;29(6-7):278-87.
34. Inugala S, Eedara BB, Sunkavalli S, Dhurke R, Kandadi P, Jukanti R, *et al.* Solid self-nanoemulsifying drug delivery system (S-SNEDDS) of darunavir for improved dissolution and oral bioavailability: *In vitro* and *in vivo* evaluation. *Eur J Pharm Sci* 2015;74:1-10.
35. Narkhede RS, Gujar KN, Gambhire VM. Design and evaluation of solid self-nanoemulsifying drug delivery systems (S-SNEDDS) for Nebivolol Hydrochloride. *Asian J Pharm* 2014;4(2):224-37.
36. Bali V, Ali M, Ali J. Nanocarrier for the enhanced bioavailability of a cardiovascular agent: *in vitro*, pharmacodynamic, pharmacokinetic and stability assessment. *Int J Pharm* 2010;403(1-2):46-56.
37. Rahman MA, Iqbal Z, Hussain Z. Formulation optimization and *in vitro* characterization of sertraline loaded self-nano-emulsifying drug delivery system for oral administration. *J Pharm Investig* 2012;42:191-202.
38. Gupta S, Chavhan S, Sawant K. Self-Nano emulsifying drug delivery system for adefovir dipivoxil: design, characterization, *in vitro* and *ex vivo* evaluation. *Colloids Surf A Physicochem Eng Asp* 2011;392(1):145-55.
39. Katteboina S, Chandrasekhar V, Balaji S. Approaches for the development of solid self-emulsifying drug delivery systems and dosage forms. *Asian J Pharm Sci* 2009;4(4):240-53.
40. Dixit RP, Nagarsenker MS. Self-nano emulsifying granules of ezetimibe: design, optimization and evaluation. *Eur J Pharm Sci* 2008;35(3):183-92.
41. Moura F, Lago R. Catalytic growth of carbon nanotubes and nanofibers on vermiculite to produce floatable hydrophobic "nanosponges" for oil spill remediation. *Appl Catal B Environ* 2009;90:436-40.
42. Arkas M, Allabashi R, Tsiourvas D, Mattausch EM, Perfle R. Organic/inorganic hybrid filters based on dendritic and cyclodextrin "nanosponges" for the removal of organic pollutants from water. *Environ Sci Technol* 2006;40(8):2771-7.
43. Darandale SS, Vavia PR. Cyclodextrin based nanosponges of Curcumin: formulation and physicochemical characterization. *J Incl Phenom Macrocycl Chem* 2013;75:315-22.
44. Rao M, Bajaj A, Pardeshi A, Aghav S. Investigation of nonporous colloidal carrier for solubility enhancement of Cefpodoxime proxetil. *J Pharm Res* 2012;5(5):2496-99.
45. Swaminathan S, Pastero L, Serpe L, Trotta F, Vavia P, Aquilano D, *et al.* Cyclodextrin-based nanosponges encapsulating camptothecin: Physicochemical characterization, stability and cytotoxicity. *Eur J Pharm Biopharm* 2010;74:193-201.
46. Rao MR, Bhingole RC. Nanosponge based pediatric-controlled release dry suspension of Gabapentin for reconstitution. *Drug Dev Ind Pharm* 2015;41(12):1-8.
47. Rao M, Bajaj A, Khole I, Munjapara G, Trotta F. *In vitro* and *in vivo* evaluation of  $\beta$ -cyclodextrin based nanosponges of Telmisartan. *J Incl Phenom Macrocycl Chem* 2013;77(1-4):135-45.
48. Bansal T, Akhtar N, Jaggi M, Khar R, Talegaonkar S. Novel formulation approaches for optimizing the delivery of anti-cancer drugs based on p-glycoprotein modulation. *Drug Discov Today* 2009;14(21-22):1067-74.
49. Sinko PJ. Martin's Physical Pharmacy and Pharmaceutical Sciences in Colloids. 5th ed. Maryland: Lippincott Williams and Wilkins; 2010. p. 469.
50. Cesar P, Quelian A, Tássia H, Blanca E, Fernando L. Evaluation and study of mebendazole polymorphs present in raw materials and tablets available in the Brazilian pharmaceutical market. *J Appl Pharm Sci* 2014;4(11):001-007.
51. Kumar M, Pathak K, Misra A. Formulation and characterization of Nano emulsion-based drug delivery system of risperidone. *Drug Dev Ind Pharm* 2009;35(4):387-95.
52. Bajaj A, Rao MR, Khole I, Munjapara G. Self-nanoemulsifying drug delivery system of cefpodoxime proxetil containing tocopherolpolyethylene glycol succinate. *Drug Dev Ind Pharm* 2013;39(5):635-45.
53. Avachat AM, Patel VG. Self-nano-emulsifying drug delivery system of stabilized ellagic acid-phospholipid complex with improved dissolution and permeability. *Saudi Pharm J* 2015;23(3):276-89.
54. Gupta S, Kesala R, Omri A. Formulation strategies to improve the bioavailability of poorly absorbed drug with special emphasis on self-emulsifying system. *ISRN Pharm* 2013;2013:848083.
55. Reddy H, Murthy R. Lymphatic transport of orally administered drug. *Indian J Exp Biol* 2002;40:1097-109.
56. Barnes G, Ian G. Interfacial Science: An Introduction. 2nd ed. Oxford, United Kingdom: Oxford University Press; 2011. p. 319.